

# Pressure solution and viscous compaction in sedimentary basins

A. C. Fowler and Xinshe Yang

Mathematical Institute, Oxford University, Oxford, England

**Abstract.** Mathematical models of compaction in sedimentary basins typically assume a relationship between effective pressure  $p_e$  and porosity  $\phi$ , which is of a non-linear type; that is,  $p_e = p_e(\phi)$ . However, at depths greater than a kilometer, pressure solution becomes important and this relationship approaches a viscous one. We derive a mathematical model for viscous compaction in sedimentary basins and show how the model suggests different styles of behavior in the limits of slow and fast compaction.

## 1. Introduction

Sedimentary basins evolve over millions of years and are of commercial and scientific interest because of their importance as sources of hydrocarbons. A practical problem of some interest in oil drilling operations is the occurrence of abnormal pore fluid pressures within the sediments. By normal pore pressures, we mean that the fluid pressure increases hydrostatically with depth, whereas abnormal fluid pressures are those in excess of this. The mechanism whereby overpressures are generated is of concern, because in drilling, the borehole is filled with a mud whose density is chosen to balance the pore pressure: if the mud density is too low, the hole will collapse, whereas if it is too high, the surrounding rock can be hydrofractured. Sudden changes in pore pressure can therefore cause blowouts or other damage. Overpressuring is associated with the time it takes for sediments to compact under their own weight. If ten kilometers of sediments are deposited very rapidly, then the initial pore pressure will be lithostatic. Over time, the sediments compact, and the resultant expulsion of pore water allows the pore pressure to approach a hydrostatic limit, and in so doing the porosity is reduced. At depths up to about a kilometer, this compaction is elastic, and due to the rearrangement of sediment particles. At greater depths, cementation and pressure solution occur, and the latter causes further compaction; we call compaction by pressure solution viscous compaction, and it forms the subject of the present paper.

One of the interesting features of overpressuring is that it typically occurs suddenly at depths in excess of 3000 meters [Hunt, 1990] and is often associated

with the formation of seals [Hunt, 1990; Bradley, 1975], which are thought to be associated with mineralization of, for example, calcite. Our concern in this paper, however, is not with the mechanics of seal formation, but with a quantitative description of how the balance between compaction and pore water expulsion can cause a relatively sudden transition between normally pressured and overpressured regions.

Studies of compaction and the overpressuring phenomenon were initiated by Athy [1930] and Hedberg [1936], and more recently, mathematical models have been developed by Smith [1971], Keith and Rimstidt [1985], Shi and Wang [1986], and Wangen [1992]. The phenomenon is related to consolidation in soils [Gibson *et al.*, 1991], and the basic governing equation is a Richards type nonlinear diffusion equation if the deformational response is nonlinear elastic.

More specifically, consolidation suggests the use of a compaction law which relates the effective pressure  $p_e$  (overburden minus pore pressure) to the sediment porosity, and early studies [Smith, 1971] use a compaction law of the form  $p_e = p_e(\phi)$ , where  $\phi$  is the porosity. Although near-surface sediments can be expected to obey this kind of law, processes of diagenesis and pressure solution begin to occur at depths greater than a kilometer, and these mechanisms may alter the rheology from an elastic one to a viscous one.

Angevine and Turcotte [1983] studied the role of pressure solution in the compaction of sediments, and this work was extended by Birchwood and Turcotte [1994]. In this paper, we develop an approach initiated by Audet and Fowler [1992] and Fowler and Yang [1998], who studied one-dimensional compaction of a sedimentary basin in a model which allowed pore fluid expulsion from the elastically compacting sediments. They found that the resulting behavior depended critically on a parameter  $\lambda$ , which represents the ratio of the hydraulic conductivity and the sedimentation rate; in particular they were able to give analytic solutions de-

Copyright 1999 by the American Geophysical Union.

Paper number 1998JB900029.

0148-0227/99/1998JB900029\$09.00

scribing the behaviour when  $\lambda \gg 1$  ('fast' compaction) and  $\lambda \ll 1$  (slow compaction).

In this paper, we seek to derive and analyze a comparable model, to describe the evolution of porosity and pore fluid pressure when the sediments compact viscously, through the mechanism of pressure solution. Pressure solution (see Figure 1) refers to a process whereby grains dissolve at intergranular contacts under non-hydrostatic stress and precipitate in the pore space. The resulting recrystallization is a mechanism whereby compaction can occur [Tada and Siever, 1989]. In the following section, we propose the general form of mathematical model which describes the compaction of porous media. The pressure solution compaction law is derived in section 3. In section 4, we nondimensionalize and simplify the model, finding that the compactional response is determined by a dimensionless parameter  $\lambda$ . Sections 5 and 6 then give numerical and analytic solutions in the two cases  $\lambda \ll 1$  and  $\lambda \gg 1$ , and a discussion of the results follows in section 7.

### 2. Mathematical Model

The sedimentary basin is characterized by a porosity  $\phi$ , and separate liquid and solid velocities  $\mathbf{u}^l$  and  $\mathbf{u}^s$ . The liquid has a pore pressure  $p^l$ , while the whole medium (liquid-solid composite) has a stress tensor  $\sigma$  (the sign convention used is that for fluids).

The basic equations [Audet and Fowler, 1992] are those of mass and momentum conservation. Mass conservation for the solid and liquid phases respectively are given by

$$\frac{\partial}{\partial t}(1 - \phi) + \nabla \cdot [(1 - \phi)\mathbf{u}^s] = 0, \tag{1}$$

$$\frac{\partial \phi}{\partial t} + \nabla \cdot [\phi\mathbf{u}^l] = 0; \tag{2}$$

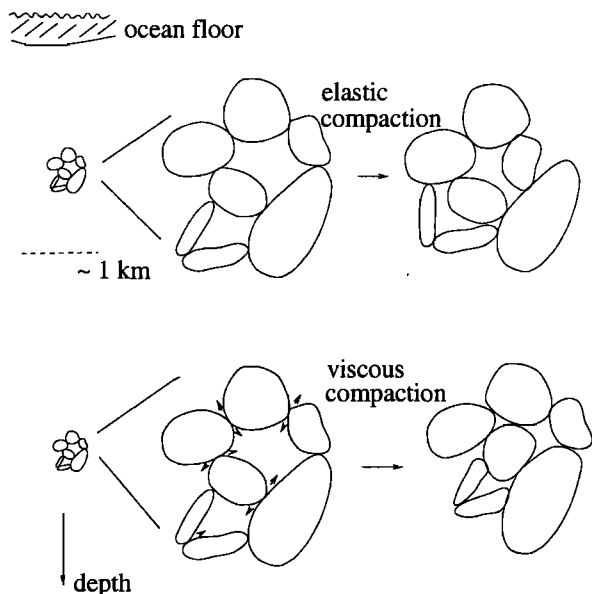


Figure 1. A schematic illustration of elastic and viscous compaction in a sedimentary basin.

liquid momentum conservation is described by Darcy's law:

$$\phi(\mathbf{u}^l - \mathbf{u}^s) = -\frac{k}{\mu}[\nabla p^l + \rho_l g \mathbf{k}], \tag{3}$$

where  $k$  is permeability,  $\mu$  is liquid viscosity,  $\rho_l$  is liquid density, and  $g$  is gravity ( $\mathbf{k}$  is a unit vector upward). Finally, medium momentum conservation for slow flow is described by a force balance:

$$\nabla \cdot \sigma - \rho g \mathbf{k} = 0, \tag{4}$$

where

$$\rho = \rho_l \phi + \rho_s(1 - \phi) \tag{5}$$

is the medium density and  $\rho_s$  is the solid density.

The equations must be supplemented by constitutive relations for  $p^l$  and  $\sigma$ , and these are respectively the compaction law and the medium rheology: they are discussed in section 3. Note that these two relations are distinct. A precise analogy is to the prescription of bulk viscosity as well as the shear viscosity in a viscous fluid [Batchelor, 1967, pp. 154, 253]. In writing (1) and (2), we assume that precipitation occurs locally; this has been shown to be a reasonable assumption by Yang [1997]. We defer a discussion of boundary conditions until a one-dimensional model is derived in section 4.

### 3. Pressure Solution and Compaction

A central concept in the dynamics of uncemented sediments is the effective stress, introduced into the soil mechanics literature by Terzaghi [1943]. Terzaghi's principle states that deformation of the sediments is determined by the effective stress, which can be defined as follows. Suppose that  $a$  is the specific interfacial grain contact area, that is, the ratio of grain surface area (per unit volume) in contact with other grains to the total grain surface area. Then  $1 - a$  is the specific grain-pore fluid interfacial contact area, and  $(1 - a)p^l$  is the pore fluid pressure exerted on the grains. Now the confining pressure  $P$  is partitioned between the solid and liquid phases, and therefore the effective pressure which acts on the solid grains, and which therefore is responsible for deformation of the solid matrix, is given by

$$p_e = P - (1 - a)p^l. \tag{6}$$

Derivation of this relation is lucidly discussed by Skempton [1960] [see also Bear and Bachmat, 1990]. Terzaghi assumed  $a = 0$ , which may be appropriate for soils, but is less so for compacting sediments. Nevertheless, Skempton [1960] suggested that typical values of  $a$  were small, and we henceforth choose  $a = 0$ .

More generally, we define the effective stress  $\sigma^e$  as (with  $a = 0$ )

$$\sigma^e = \sigma + p^l \delta, \tag{7}$$

where  $\delta$  represents the unit tensor: if we extend Terzaghi's principle to a viscously compacting medium, it is natural to suppose that the constitutive relation relates

the effective stress to the (solid) strain rate. Thus we pose a rheological constitutive law in the form

$$\sigma_{ij}^e + p_e \delta_{ij} = 2\eta(\dot{\epsilon}_{ij} - \frac{1}{3}\nabla \cdot \mathbf{u}^s \delta_{ij}), \tag{8}$$

where  $\eta$  is the medium viscosity and the solid strain rate tensor is

$$\dot{\epsilon}_{ij} = \frac{1}{2} \left( \frac{\partial u_i^s}{\partial x_j} + \frac{\partial u_j^s}{\partial x_i} \right). \tag{9}$$

The prescription of the effective shear viscosity  $\eta$  depends on the rate of pressure solution creep at the grain scale. In addition, this also determines the compaction law. *Weyl* [1959] and *Rutter* [1976] derived a creep law to describe pressure solution (of quartz), in the form of a relation between the solid dilation rate and the effective pressure on the grains. Following *Lahner* [1995], we write this as

$$-\dot{\epsilon}_{ii} = \frac{A\nu_m M_s c_0 w D_{gb}}{RT \rho_s \bar{d}^3} p_e, \tag{10}$$

where the summation convention is used ( $\dot{\epsilon}_{ii} = \text{tr } \dot{\epsilon}_{ij}$ ), and where  $A$  is a constant,  $\nu_m$  is the molar volume of water,  $c_0$  is the (equilibrium) concentration of quartz in the pore fluid,  $M_s$  is the molecular weight of quartz,  $\bar{d}$  is the average grain diameter,  $D_{gb}$  is the grain boundary diffusion coefficient along grain contact boundaries of width  $w$ ,  $R$  is the gas constant, and  $T$  is absolute temperature. Thus the pressure solution compaction law is

$$p_e = -\xi \nabla \cdot \mathbf{u}^s, \tag{11}$$

where

$$\xi = \frac{\rho_s RT \bar{d}^3}{A\nu_m M_s c_0 w D_{gb}}. \tag{12}$$

This is analogous to creep controlled viscous compaction laws used in studies of magma transport in the Earth's mantle [*McKenzie*, 1984, *Fowler*, 1990], and suggests that the medium viscosity  $\eta$  is related to the compaction viscosity  $\xi$ ; *Fowler* [1990] suggested that  $\xi \approx \eta/\phi$ , for example [cf. *Batchelor*, 1967, p. 253].

### 4. A Reduced, One-Dimensional Model

Compaction is essentially a one-dimensional phenomenon: variations in the horizontal are much slower than in the vertical because of the large aspect ratio of typical sedimentary basins. If  $z$  represents the vertical coordinate upward, and if we now suppose the velocities are purely vertical (horizontal strain rates are zero), then (1)–(3) are simply

$$\begin{aligned} -\frac{\partial \phi}{\partial t} + \frac{\partial}{\partial z} [(1 - \phi)u^s] &= 0, \\ \frac{\partial \phi}{\partial t} + \frac{\partial}{\partial z} [\phi u^l] &= 0, \\ \phi(u^l - u^s) &= -\frac{k}{\mu} \left[ \frac{\partial p^l}{\partial z} + \rho_l g \right]. \end{aligned} \tag{13}$$

The compaction law is

$$p_e = -\xi \frac{\partial u^s}{\partial z}, \tag{14}$$

and the medium force balance (4) can be written, using (10) and (11), as

$$\frac{4}{3} \frac{\partial}{\partial z} \left( \eta \frac{\partial u^s}{\partial z} \right) - \frac{\partial p_e}{\partial z} - \frac{\partial p^l}{\partial z} - \rho g = 0. \tag{15}$$

We suppose that the sediments lie in  $0 < z < h(t)$ , with  $z = 0$  being an impermeable basement. Suitable boundary conditions are then

$$u^s = u^l = 0 \text{ at } z = 0, \tag{16}$$

and

$$p_e = p^l = 0, \quad \dot{h} = v_s + u^s \text{ at } z = h(t). \tag{17}$$

We take the pressures to be measured relative to a reference pressure, which is equal to the fluid pressure at  $z = h$ . The constant  $\phi_0$  is the initial settlement porosity, and the relation for  $\dot{h}$  is a kinematic condition which includes the sediment deposition rate  $v_s$  (given as a velocity; specifically, if  $\dot{m}_s$  is the sedimentation rate in units of mass per unit area per unit time, then  $v_s = \dot{m}_s / \rho_s \phi_0$ ).

#### 4.1. Nondimensionalization

Sedimentary basins have typical depths in the range 1–10 km. For a particular basin the depth scale  $d$  can then be taken to be the average depth; then  $d/[v_s]$  is a suitable timescale, where  $[v_s]$  represents a typical value of the (possibly variable)  $v_s$ . Using (14) and (15) (and taking  $\eta$  as constant) we can eliminate  $p^l$  to obtain (13) in the form

$$\begin{aligned} -\phi(u^l - u^s) &= \\ -\frac{k}{\mu} \left[ \left( \frac{4\eta}{3\xi} + 1 \right) \frac{\partial p_e}{\partial z} + (\rho_s - \rho_l)(1 - \phi)g \right], \end{aligned} \tag{18}$$

and adding (13)<sub>1</sub> and (13)<sub>2</sub> (the subscripted equation numbers refer to the first and second equations in the display (13), respectively) and integrating, (using (16)), we have

$$-\phi(u^l - u^s) = u^s. \tag{19}$$

We now choose a pressure scale to be  $[p] = (\rho_s - \rho_l)gd / [4\eta/3\xi + 1]$ , and write the variables as

$$\begin{aligned} p_e &= (\rho_s - \rho_l)gd \left[ \frac{4\eta}{3\xi} + 1 \right]^{-1} p, \\ u^s &= [v_s]u, \\ z &= dz^*, \\ t &= (d/[v_s])t^*, \\ h &= dh^*, \\ v_s &= [v_s]v_s^*, \\ k &= k_0 \tilde{k}, \end{aligned} \tag{20}$$

where we define  $k_0$  to be the permeability at  $z = h$ , where  $\phi = \phi_0$ , so that  $\tilde{k} = 1$  when  $\phi = \phi_0$ . The dimensionless model can be written (using (18)) as

$$\begin{aligned}
 -\frac{\partial \phi^*}{\partial t^*} + \frac{\partial}{\partial z^*} [(1 - \phi^*)u^*] &= 0, \\
 u^* &= -\lambda \tilde{k} \left[ \frac{\partial p^*}{\partial z^*} + 1 - \phi^* \right], \\
 p^* &= -\Xi \frac{\partial u^*}{\partial z^*}.
 \end{aligned}
 \tag{21}$$

Following *Smith* [1971], we choose

$$\tilde{k} = (\phi/\phi_0)^m, \tag{22}$$

with a typical value of  $m = 8$ . This large value is of crucial significance later. The dimensionless parameters are given by

$$\lambda = \frac{k_0(\rho_s - \rho_l)g}{\mu[v_s]}, \tag{23}$$

or  $\lambda = K/[v_s]$ , where  $K$  is the hydraulic conductivity; also

$$\Xi = \frac{\xi[v_s]}{(\rho_s - \rho_l)gd^2} \left( \frac{4\eta}{3\xi} + 1 \right). \tag{24}$$

The parameter  $\lambda$  measures the ratio of the Darcy flow rate to the sedimentation rate. Large values of  $\lambda$  indicate rapid compaction, or slow sedimentation. A typical value of  $v_s$  is  $10^{-11} \text{ m s}^{-1}$  ( $300 \text{ m Ma}^{-1}$ ), while  $K$  may range from as much as  $10^{-2} \text{ m s}^{-1}$  for clean sand to  $10^{-13} \text{ m s}^{-1}$  for shale or marine clay [*Freeze and Cherry, 1979*]. Thus  $10^{-2} < \lambda < 10^9$ ; small or large values of  $\lambda$  may occur, with large values being perhaps of greater significance.

**4.2. Values of Parameters**

The parameter  $\Xi$  measures the efficiency of compaction. In terms of the effective pressure scale  $[p]$ ,  $\Xi = \xi[v_s]/[p]d$ . Now the compaction law can be written in the dimensional form

$$\frac{d\phi}{dt_s} = -\frac{(1 - \phi)p_e}{\xi}, \tag{25}$$

where  $d/dt_s$  is a material derivative following the solid matrix. Since, by choice,  $d$  is a depth scale over which significant variations of  $\phi$  occur and since  $d/[v_s]$  is the timescale on which this occurs, this suggests that  $[v_s]/d = O([p]/\xi)$  and thus that  $\Xi = O(1)$ . In fact, we could choose  $d$  by prescribing  $\Xi = 1$ . In fact, if we use typical values [*Rutter, 1976; Gratz, 1991; Birchwood and Turcotte, 1994*]

$$\begin{aligned}
 \rho_s &= 2.5 \times 10^3 \text{ kg m}^{-3}, \quad R = 8.3 \text{ J mol}^{-1} \text{ K}^{-1}, \\
 T &= 300 \text{ K}, \quad M_s = 6 \times 10^{-2} \text{ kg mol}^{-1}, \\
 \nu_m &= 2 \times 10^{-5} \text{ m}^3 \text{ mol}^{-1}, \quad wD_{gb} = 10^{-19} \text{ m}^3 \text{ s}^{-1}, \\
 \bar{d} &= 10^{-4} \text{ m}, \quad c_0 = 10^{-4} \text{ M}, \quad A = 16,
 \end{aligned}
 \tag{26}$$

we find  $\xi \sim 3 \times 10^{22} \text{ Pa s}$ , a value comparable to inferred estimates of the viscosity of the Earth's mantle [*Turcotte and Schubert, 1982*]. If we take  $[v_s] = 10^{-11} \text{ m s}^{-1}$ ,  $\rho_s - \rho_l \sim 1.5 \times 10^3 \text{ kg m}^{-3}$ ,  $g = 10 \text{ m s}^{-2}$ ,  $d = 5 \text{ km}$ ,  $1 + (4\eta/3\xi) \approx 1.5$ , then indeed (24) implies  $\Xi \approx 1$ . Since, in assessing field data, we would typically specify  $d$  as the basin depth, we leave  $\Xi$  as a parameter in the model and will assume it be of  $O(1)$ .

Boundary conditions for (21) are that

$$\begin{aligned}
 u^* &= 0 \quad \text{on } z^* = 0, \\
 p^* &= 0, \quad \phi = \phi_0, \\
 \dot{h}^* &= v_s^* + u^* \quad \text{at } z^* = h^*(t^*).
 \end{aligned}
 \tag{27}$$

**5. Slow Compaction:  $\lambda \ll 1$**

For convenience, we henceforward omit the asterisks on the dimensionless variables. Figure 2 shows a numerical solution of the model when  $\lambda = 0.01$ . Just as for the case of elastic compaction [*Fowler and Yang, 1998*], a boundary layer forms at the base, in which compaction occurs. For  $\lambda \ll 1$ , we see that  $u = O(\lambda)$ , whence  $\partial\phi/\partial t = O(\lambda)$  and  $\phi \approx \phi_0$  everywhere. Thus  $\tilde{k} \approx 1$ , and  $u$  satisfies

$$u = -\lambda \left[ -\Xi \frac{\partial^2 u}{\partial z^2} + 1 - \phi_0 \right], \tag{28}$$

with suitable boundary conditions representing the boundary layer matching to the far field solution  $u = -\lambda(1 - \phi_0)$  being

$$\begin{aligned}
 u &= 0 \quad \text{on } z = 0, \\
 u &\rightarrow -\lambda(1 - \phi_0) \quad \text{as } z \rightarrow \infty.
 \end{aligned}
 \tag{29}$$

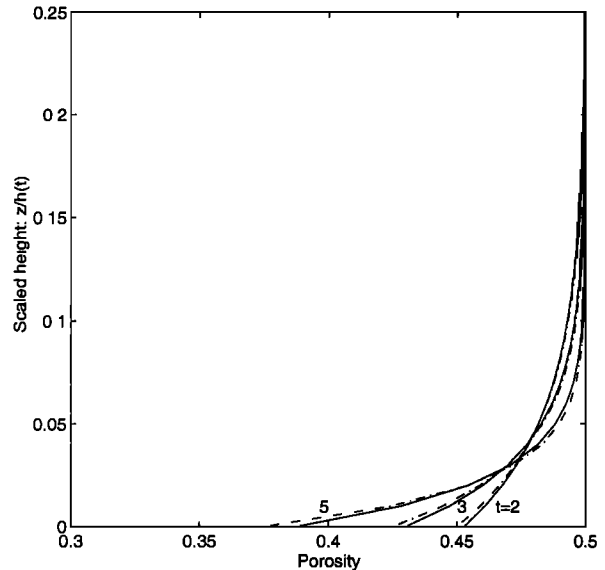


**Figure 2.** Numerical solution of (21) and (27) with  $\lambda = 0.01$ ,  $\Xi = 1$ ,  $v_s = 1$ , and  $\tilde{k} = (\phi/\phi_0)^m$  with  $m = 8$ . Profiles of  $\phi$  near the base are shown at times  $t = 2, 3, 5$ , together with the analytic approximations (dashed) determined from (31)

The solution is

$$u = -\lambda(1 - \phi_0)\{1 - \exp[-z/(\lambda \Xi)^{1/2}]\}, \quad (30)$$

and the correction for  $\phi$  is then found to be

$$\phi = \phi_0 - (1 - \phi_0)^2 \left(\frac{\lambda}{\Xi}\right)^{1/2} t \exp[-z/(\lambda \Xi)^{1/2}], \quad (31)$$

with  $h$  being given (for constant  $v_s$ ) by

$$h \approx [v_s - \lambda(1 - \phi_0)]t. \quad (32)$$

The accuracy of the approximation in the boundary layer breaks down when  $(\phi/\phi_0)^m < 1$ ; since  $(\phi/\phi_0) = 1 - O(\lambda^{1/2}t)$ , this is when  $t = O(1/m\lambda^{1/2})$ ; for  $m = 8$  and  $\lambda = 10^{-2}$ , this is  $O(1)$ , but in fact (31) is quite accurate even up to  $t = 5$ . Just as for the elastic case, slow viscous compaction limits compaction to a basal boundary layer. In the elastic case, this boundary layer grows diffusively; in the viscous case, it is essentially stationary.

### 6. Fast Compaction: $\lambda \gg 1$

The case where  $\lambda \gg 1$  is of greater complexity and interest. Figure 3 shows the evolution of the porosity profile with time. The most prominent feature is the apparent relaxation of  $\phi$  near  $z = h$  to a concave function of the depth  $h - z$ . In contrast, elastic compaction leads to an exponential function of depth [Fowler and Yang, 1998].

We can understand this as follows. First, it is convenient to define a critical porosity  $\phi^*$  by

$$\phi^* = \phi_0 \exp\left[-\frac{1}{m} \ln \lambda\right]. \quad (33)$$

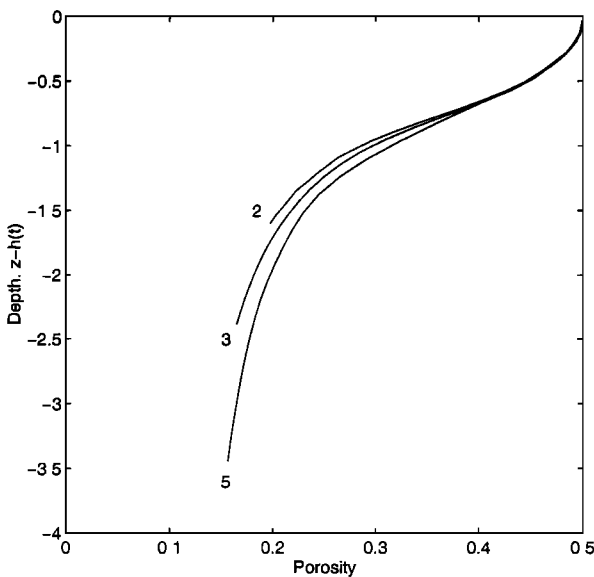


**Figure 3.** Evolution of porosity profile with time, plotted as a function of depth  $h - z$ . Parameters are the same as for figure 1, but  $\lambda = 100$ .

Although formally  $\phi^* \ll 1$  for  $\lambda \gg 1$ , in practice  $\phi^* = O(1)$  if  $m$  is large. For  $\lambda = 10^2$ ,  $m = 8$ , and  $\phi_0 = 0.5$ , we get  $\phi^* = 0.28$ . Even for  $\lambda = 10^6$ ,  $\phi^* = 0.08$ . The equations (21) are

$$\begin{aligned} -\frac{\partial \phi}{\partial t} + \frac{\partial}{\partial z}[(1 - \phi)u] &= 0, \\ u &= -\left(\frac{\phi}{\phi^*}\right)^m \left[\frac{\partial p}{\partial z} + 1 - \phi\right], \\ p &= -\Xi \frac{\partial u}{\partial z}, \end{aligned} \quad (34)$$

with the boundary conditions (27) (and we take  $v_s$  as constant). We assume  $\phi^* = O(1)$  and  $m \gg 1$ .

So long as  $\phi > \phi^*$ , then  $(\phi/\phi^*)^m$  is exponentially large (because  $m$  is large), and (34)<sub>2</sub> then implies

$$\phi \approx 1 + \frac{\partial p}{\partial z}. \quad (35)$$

Substituting this into the  $\phi$  equation (34)<sub>1</sub> gives

$$\frac{\partial^2 p}{\partial z \partial t} + \frac{\partial}{\partial z} \left[ u \frac{\partial p}{\partial z} \right] = 0; \quad (36)$$

Integrating with respect to  $z$ , using  $p = 0$  on  $z = h$ , whence (on  $z = h$ )  $p_t + up_z = (u - \dot{h})p_z = (h - u)(1 - \phi_0)$  from (35) (and  $\phi = \phi_0$ ),  $= v_s(1 - \phi_0)$  using (27), we obtain

$$\frac{\partial p}{\partial t} + u \frac{\partial p}{\partial z} = v_s(1 - \phi_0), \quad (37)$$

a hyperbolic equation for  $p$  with characteristic speed  $u < 0$ . We solve (37) with  $p = 0$  on  $z = h$ , together with

$$p = -\Xi \frac{\partial u}{\partial z} \quad (38)$$

with  $u = 0$  on  $z = 0$ , so long as  $\phi$  given by (35) is  $> \phi^*$ . We solve (37) by the method of characteristics, which gives

$$\begin{aligned} p &= v_s(1 - \phi_0)(t - \tau), \\ z &= \int_{\tau}^t u(s, \tau) ds + h(\tau), \end{aligned} \quad (39)$$

and determines  $p$  implicitly in terms of the parameter  $\tau$ , and the as yet unknown functions  $h$  and  $u$ .

If we change coordinates from  $(z, t)$  to  $(t, \tau)$ , we find

$$\begin{aligned} \frac{\partial u}{\partial z} &= \frac{\partial u}{\partial \tau} \bigg/ \frac{\partial z}{\partial \tau}, \\ \frac{\partial z}{\partial \tau} &= v_s + \int_{\tau}^t \frac{\partial u}{\partial \tau}(s, \tau) ds. \end{aligned} \quad (40)$$

Thus (38) can be written in the form

$$\frac{v_s(1 - \phi_0)(t - \tau)}{\Xi} = \frac{-u_{\tau}}{v_s + \int_{\tau}^t u_{\tau}(s, \tau) ds}, \quad (41)$$

which can be integrated with respect to  $t$  to yield

$$\int_{\tau}^t u_{\tau}(s, \tau) ds = v_s \left\{ \exp \left[ \frac{-v_s(1 - \phi_0)(t - \tau)^2}{2\Xi} \right] - 1 \right\}. \quad (42)$$

We substitute this expression into (41) and integrate with respect to  $\tau$ , to find

$$u = \dot{h}(t) - v_s \exp \left[ \frac{-v_s(1 - \phi_0)(t - \tau)^2}{2\Xi} \right]. \quad (43)$$

Now we substitute (43) into (39)<sub>2</sub>, to find

$$h(\tau) - z = \int_{\tau}^t \left\{ v_s \exp \left[ \frac{-v_s(1 - \phi_0)(s - \tau)^2}{2\Xi} \right] - \dot{h}(s) \right\} ds. \quad (44)$$

Simplification of this expression yields

$$h(t) - z = \left( \frac{\Xi v_s \pi}{2(1 - \phi_0)} \right)^{1/2} \operatorname{erf} \left[ \left( \frac{v_s(1 - \phi_0)}{2\Xi} \right)^{1/2} (t - \tau) \right]. \quad (45)$$

We thus have  $p$  in (39)<sub>1</sub>,  $u$  in (43), and  $h - z$  given as explicit functions of  $t - \tau$  (and  $h$ ). In particular,  $t - \tau$  depends only on depth  $h - z$ , hence so does  $p$ , and so therefore does  $\phi$  (from (35)). Therefore  $\phi_t = -h\phi_z$ , and (34)<sub>1</sub> gives, on integrating and using (27) and (43),

$$\phi = 1 - (1 - \phi_0) \exp \left[ \frac{v_s(1 - \phi_0)}{2\Xi} (t - \tau)^2 \right]. \quad (46)$$

For small depths,  $t - \tau \propto h - z$ , and thus  $\phi = \phi_0 - O[(h - z)^2]$ , as we can see in figure 3.

It only remains to choose  $h$  so as to satisfy  $u = 0$  on  $z = 0$ . If  $t = t_b(\tau)$  at  $z = 0$ , then (39)<sub>2</sub> and (43) imply

$$\begin{aligned} h(\tau) &= - \int_{\tau}^{t_b(\tau)} u(s, \tau) ds, \\ \dot{h}[t_b(\tau)] &= v_s \exp \left[ \frac{-v_s(1 - \phi_0)[t_b(\tau) - \tau]^2}{2\Xi} \right]. \end{aligned} \quad (47)$$

Using (43) in (47)<sub>1</sub> gives

$$h[t_b(\tau)] = v_s \int_{\tau}^{t_b(\tau)} \exp \left[ \frac{-v_s(1 - \phi_0)(s - \tau)^2}{2\Xi} \right] ds. \quad (48)$$

Equation (48) simplifies to

$$\begin{aligned} &\left( \frac{v_s(1 - \phi_0)}{2\Xi} \right)^{1/2} [t_b(\tau) - \tau] \\ &= \operatorname{erf}^{-1} \left\{ \left[ \frac{2(1 - \phi_0)}{v_s \Xi \pi} \right]^{1/2} h[t_b(\tau)] \right\}, \end{aligned} \quad (49)$$

so that together with (47)<sub>2</sub>, we obtain

$$\dot{h} = v_s \exp \left[ - \left( \operatorname{erf}^{-1} \left\{ \left[ \frac{2(1 - \phi_0)}{v_s \Xi \pi} \right]^{1/2} h \right\} \right)^2 \right] \quad (50)$$

as the evolution equation for  $h$ . Together with (50), we gather the solutions for  $p$ ,  $h - z$ ,  $\phi$ , and  $u$  together here. With  $A = v_s(1 - \phi_0)/2\Xi$ , and  $\zeta = t - \tau$ , they are

$$\begin{aligned} \phi &= 1 - (1 - \phi_0) \exp[A\zeta^2], \\ h - z &= \frac{v_s}{2} \sqrt{\frac{\pi}{A}} \operatorname{erf}[A^{1/2}\zeta], \\ u &= \dot{h} - v_s \exp[-A\zeta^2], \\ p &= 2\Xi A \zeta, \end{aligned} \quad (51)$$

and the solution of (50) is

$$h = \frac{v_s}{2} \left( \frac{\pi}{A} \right)^{1/2} \operatorname{erf}[A^{1/2}t]. \quad (52)$$

Notice that (52) implies a maximum  $h$  equal to  $h_{\max} = [v_s \Xi \pi / 2(1 - \phi_0)]^{1/2} = (v_s/2)(\pi/A)^{1/2}$ . Now the solution (51) becomes invalid if  $\phi$  reaches  $\phi^*$ , i.e., when

$$A\zeta^2 = \ln \left[ \frac{1 - \phi^*}{1 - \phi_0} \right]. \quad (53)$$

This first occurs at  $z = 0$  when  $h = h^*$  given by

$$h^* = \frac{v_s}{2} \sqrt{\frac{\pi}{A}} \operatorname{erf} \left\{ \left[ \ln \left( \frac{1 - \phi^*}{1 - \phi_0} \right) \right]^{1/2} \right\}. \quad (54)$$

Since the error function is less than one,  $h^* < h_{\max}$ , and the breakdown will always eventually occur.

If we define

$$\zeta^* = \left\{ \frac{1}{A} \ln \left( \frac{1 - \phi^*}{1 - \phi_0} \right) \right\}^{1/2} \quad (55)$$

as the value in (53) where breakdown occurs, then we have from (51) and (52) that breakdown first occurs at  $t = \zeta^*$ , and thereafter it occurs at a depth  $h - z = h^*$ , where  $\zeta = \zeta^*$ , and

$$\begin{aligned} u = u^* &= \dot{h} - v_s \exp[-A\zeta^{*2}], \\ p = p^* &= 2\Xi A \zeta^*. \end{aligned} \quad (56)$$

For values of  $t > \zeta^*$ , there is a transition region which can be analyzed as follows in section 6.1.

### 6.1. Transition Region

A suitable balance of terms in the transition region is effected by defining

$$\begin{aligned} \phi &= \phi^* \exp \left[ -\frac{2}{m} \ln m + \frac{\Psi}{m} \right], \\ z &= h - h^* - \frac{2}{\gamma m} \ln m + \frac{\eta}{m}, \\ u &= W/m, \end{aligned} \quad (57)$$

where

$$\gamma = \frac{\phi'^*}{\phi^*}, \quad (58)$$

$\phi'^* = \phi_z|_{z=h-h^*}$ , and from the solution (51) in  $z > h - h^*$ ,

$$\gamma = \frac{p^*(1 - \phi^*)^2}{\Xi v_s \phi^* (1 - \phi_0)}. \tag{59}$$

Matching to the variables as  $\eta \rightarrow \infty$ , where

$$\begin{aligned} \phi &\sim \phi^* + \phi'^*(z - h + h^*) \\ &\sim \phi^* \exp\left[-\frac{2 \ln m}{m} + \frac{\gamma \eta}{m}\right], \\ u &\sim u^* - \frac{p^*}{\Xi}(z - h + h^*), \\ p &\sim p^* - (1 - \phi^*)(z - h + h^*), \end{aligned} \tag{60}$$

is effected to leading order by requiring

$$\Psi \sim \gamma \eta, \quad W \sim W^* - \frac{p^*}{\Xi} \eta, \quad p \sim p^* \quad \text{as } \eta \rightarrow \infty, \tag{61}$$

where

$$u^* = -\frac{2p^*}{\gamma \Xi m} \ln m + \frac{W^*}{m} \tag{62}$$

is anticipated to be small (certainly  $u^* = 0$  at  $t = \zeta^*$ , and in fact assuming  $u^* = O(1)$  leads to inconsistency).

Changing variables to  $(t, \eta)$  via  $\partial_t \rightarrow \partial_t - m \dot{h} \partial_\eta$ ,  $\partial_z \rightarrow m \partial_\eta$ , gives, to leading order,

$$\begin{aligned} \dot{h} \phi^* \Psi_\eta + (1 - \phi^*) W_\eta &= 0, \\ W &= -p_\eta e^{-\Psi}, \\ p &= -\Xi W_\eta, \end{aligned} \tag{63}$$

and thus

$$W = W^* - \frac{\dot{h} \phi^*}{1 - \phi^*} \Psi \tag{64}$$

(this satisfies (61) in view of (59), (55), and (56), given that  $u^* \ll 1$ ), and hence

$$\Xi \Psi_{\eta\eta} = (\Psi - \Psi_\infty) e^{-\Psi}, \tag{65}$$

where

$$\Psi_\infty = \frac{(1 - \phi^*) W^*}{\dot{h} \phi^*}. \tag{66}$$

The first integral of (65) satisfying (61) is

$$\frac{1}{2} \Xi \Psi_\eta^2 + [\Psi + 1 - \Psi_\infty] e^{-\Psi} = \frac{1}{2} \Xi \gamma^2, \tag{67}$$

and in order for this to match to a feasible solution below, we require  $\Psi \rightarrow \Psi_\infty$  as  $\eta \rightarrow -\infty$ , whence (67) implies

$$\frac{1}{2} \Xi \gamma^2 = e^{-\Psi_\infty}. \tag{68}$$

This defines  $\Psi_\infty$  in terms of  $\gamma$  given by (59), hence (66) gives  $W^*$  (in terms of  $\dot{h}$ ), so that (62) gives  $u^*$ . From (55) and (56), together with (62) and (66),

$$\begin{aligned} u^* &= \dot{h} - v_s \left( \frac{1 - \phi_0}{1 - \phi^*} \right) \\ &= -\frac{2p^*}{\gamma \Xi m} \ln m + \frac{\phi^* \Psi_\infty}{m(1 - \phi^*)} \dot{h}, \end{aligned} \tag{69}$$

whence

$$\dot{h} = \frac{v_s \left( \frac{1 - \phi_0}{1 - \phi^*} \right) - \frac{2p^*}{\gamma \Xi m} \ln m}{1 - \frac{\phi^* \Psi_\infty}{m(1 - \phi^*)}}, \tag{70}$$

We note from (56) that at breakdown, when  $t = \zeta^*$ ,  $\dot{h} = v_s(1 - \phi_0)/(1 - \phi^*)$ ; (70) indicates that there is an  $O(\frac{1}{m} \ln m)$  correction to  $\dot{h}$  as  $t$  passes through  $\zeta^*$ . Figure 4 plots the numerical solution for  $h$  at  $\lambda = 100$ , compared to the approximations (52) for  $t < \zeta^*$  and (70) for  $t > \zeta^*$ .

### 6.2. Below Transition

As  $\eta \rightarrow -\infty$ , we have  $W, p \rightarrow 0$ , and  $\Psi \rightarrow \Psi_\infty$ . Reverting to the  $z$  coordinate and defining

$$W = \frac{1}{m} \hat{W}, \quad \Psi = \Psi_\infty + \frac{1}{m} \hat{\Psi}, \quad p = \frac{1}{m^2} \hat{p}, \tag{71}$$

then to leading order

$$\begin{aligned} -\phi^* \hat{\Psi}_t + (1 - \phi^*) \hat{W}_z &= 0, \\ \hat{W} &= -e^{\Psi_\infty} \left[ -\frac{1}{m^2} \Xi \hat{p}_z + 1 - \phi^* \right], \\ \hat{p} &= -\Xi \hat{W}_z. \end{aligned} \tag{72}$$

The solution is incomplete as we have not computed  $O(1/m)$  terms in the transition zone: apparently,  $\hat{\Psi} = \hat{\Psi}(z)$ ,  $\hat{W} \approx -(1 - \phi^*) e^{\Psi_\infty}$ ,  $\hat{p} \approx 0$ , and the basal boundary condition  $W = 0$  at  $z = 0$  is satisfied by a boundary layer solution

$$\hat{W} = -(1 - \phi^*) e^{\Psi_\infty} \left[ 1 - \exp\left(-\frac{\Xi^{1/2} e^{\Psi_\infty/2}}{m} z\right) \right].$$

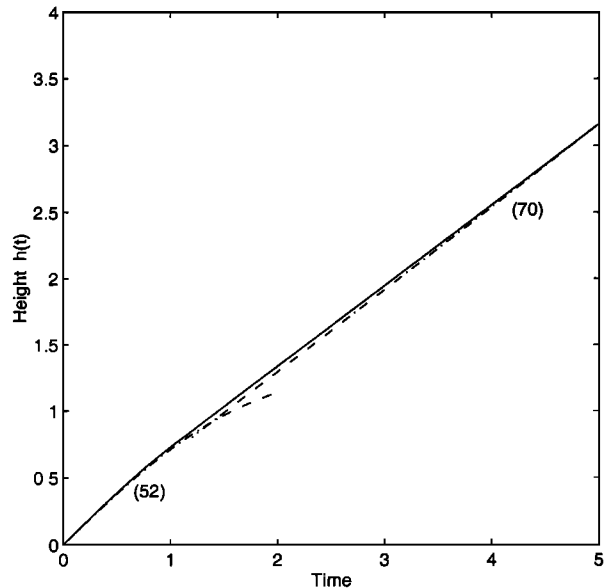


**Figure 4.** Numerical solution for  $h(t)$  when  $\lambda = 100$ , together with the approximations (52) for  $t < \zeta^*$  and (70) for  $t > \zeta^*$  (the additive constant for (70) has not been determined, whence the apparent slight jump in  $h$  near  $t = \zeta^*$ ).

This boundary layer is passive, and  $h$  is controlled by the dynamics of the transition. Figure 5 plots the numerical solution for  $\phi$ , together with the predicted solutions in the upper region and the transition zone.

## 7. Discussion

For a model of sedimentary basin formation which incorporates viscous compaction due to pressure solution, we have been able to derive approximate solutions in the distinct limits of slow compaction, where  $\lambda = K/v_s \ll 1$ ,  $K$  being the hydraulic conductivity and  $v_s$  the sedimentation rate, and fast compaction, where  $\lambda \gg 1$ . When  $\lambda \ll 1$ , compaction is limited to a basal boundary layer of thickness  $O(\sqrt{\lambda})$ . This result is similar to that which occurs for elastic compaction and is equivalent to results obtained in viscous compaction in the asthenosphere [e.g., McKenzie, 1984].

The more realistic case to consider is when  $\lambda \gg 1$ ; compaction occurs throughout the basin, and the basic equilibrium solution which applies near the surface is a near parabolic profile of porosity versus depth. In fact, for small values of  $A^{1/2}\zeta$  in (51), we have the depth

$$Z = h - z \approx v_s \zeta, \quad (73)$$

whence the porosity profile is

$$\phi \approx \phi_0 - \frac{(1 - \phi_0)^2}{2E v_s} Z^2; \quad (74)$$

this compares with the equilibrium elastic profile, which tends to be exponentially decreasing with depth. Furthermore, it is easy to show that for such small depths, the pore fluid is normally (that is, hydrostatically) pressured. The parabolic decrease of porosity is not ob-

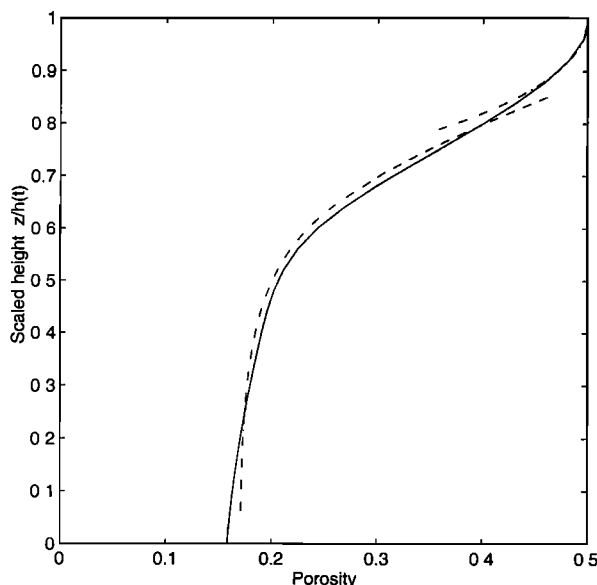


**Figure 5.** Comparison of the numerical solution (solid) for  $\lambda = 100$  at  $t = 5$ , together with the upper (equilibrium) solution and the transition solution.

served, but this is associated with the extension of the viscous compaction model all the way to the top of the basin; in our previous paper [Fowler and Yang, 1998], we showed that elastic compaction does in fact give an exponential decrease of porosity with depth.

However, this normally pressured solution is only valid to a (dimensional) depth  $h_c = dh^*$  given by (54), and approximately

$$h_c \approx \left\{ \frac{2(\frac{4}{3}\eta + \xi)v_s^D}{(\rho_s - \rho_w)g(1 - \phi_0)} \ln \left( \frac{1 - \phi^*}{1 - \phi_0} \right) \right\}^{1/2}, \quad (75)$$

where  $v_s^D$  is the dimensional sedimentation rate. Assuming  $\eta \approx \xi$ , this is roughly  $h_c \approx [\xi v_s^D / (\rho_s - \rho_w)g]^{1/2}$ . Using our previous estimates, this is 4.5 km. Note that this is *only* an estimate, as  $\xi$  is not well constrained. At this depth, the permeability has decreased sufficiently that the hydrostatic balance no longer applies, and there is a narrower transition region in which the effective pressure drops to near zero and the porosity profile changes shape. This transition region marks a (relatively sudden) switch from a normally pressured environment to one with high pore pressures and is caused by the sharp variation of permeability with porosity. Notice also that even if the permeability exponent is not large, so that  $\phi^*$  is small [ $\phi^* = \phi_0 \exp(-\frac{1}{m} \ln \lambda)$ ], nevertheless (75) (or (54)) implies that the critical depth is still finite. Thus the switch from normally pressured to abnormally pressured is predicted to occur in any case. More generally, we might therefore expect that in a marine environment where stratigraphic layers cause sudden changes in permeability, that clay layers with small permeability may be associated with the formation of abnormally high pressures.

Porosity–depth profiles (e.g., Mudford and Best, 1989; Powley, 1990) often exhibit behaviour similar to that in figure 5: decrease of porosity with depth followed by a sudden switch to a relatively uniform porosity. This switch is often associated with a jump to high pore pressures across a mineralized seal; what we have shown here is that such behaviour is intrinsic to the mechanics of a viscously compacting layer of sediments, and will always occur if the basin is deep enough, purely due to compaction: diagenesis or mineralization is not necessary.

In a previous paper, we analyzed nonlinear elastic compaction [Fowler and Yang, 1998] in which the relation between  $p_e$  and  $\phi$  was taken as

$$p_e = p_e(\phi). \quad (76)$$

Equivalently, this can be written, using (1), as

$$\nabla \cdot \mathbf{u}^s = -\frac{1}{K_e} \frac{dp_e}{dt_s}, \quad (77)$$

where  $K_e = -(1 - \phi)p'_e(\phi) > 0$  is a modulus of compression and  $d/dt_s = \partial/\partial t + \mathbf{u}^s \cdot \nabla$  is a material derivative following the solid. Contradistinctively, the viscous compaction law (11) is

$$\nabla \cdot \mathbf{u}^s = -\frac{1}{\xi} p_e. \quad (78)$$

Now pressure solution only becomes significant at depths greater than 1 km. At shallow depths, we expect elastic compaction to occur, and an obvious question is then to enquire how both mechanisms can be included. We do not pursue this too far here, but an obvious way is to generalize the above relations to a viscoelastic compaction law, here of Maxwell type:

$$\nabla \cdot \mathbf{u}^s = -\frac{1}{K_e} \frac{dp_e}{dt_s} - \frac{1}{\xi} p_e. \quad (79)$$

Equivalently, we would anticipate a viscoelastic rheology for the medium; this involves material derivatives of tensors, and some care is needed to ensure that the resulting model is frame indifferent.

At greater depths still, cementation begins to occur. As the grain boundaries begin to become cemented, pressure solution will decrease, and it can be expected that the rheology reverts to an elastic one; from the point of view of the sediments, compaction will cease and the medium will become virtually rigid, with pore pressure being controlled purely by Darcy flow. Incorporation of these and other processes such as diagenesis will form the substance of future developments.

## References

- Angevine, C.L., and D.L. Turcotte, Porosity reduction by pressure solution: a theoretical model for quartz arenites, *Geol. Soc. Am. Bull.*, *94*, 1129–1134, 1983.
- Athy, L.F., Density, porosity, and compaction of sedimentary rocks, *Am. Assoc. Petrol. Geol. Bull.*, *14*, 1–22, 1930.
- Audet, D.M., and A.C. Fowler, A mathematical model for compaction in sedimentary basins, *Geophys. J. Int.*, *110*, 577–590, 1992.
- Batchelor, G. K., *An Introduction to Fluid Dynamics*, Cambridge Univ. Press, New York, 1967.
- Bear, J., and Y. Bachmat, *Introduction to Modelling of Transport Phenomena*, Kluwer Acad., Norwell, Mass., 1990.
- Birchwood, R.A., and D.L. Turcotte, A unified approach to geopressuring, low-permeability zone formation, and secondary porosity generation in sedimentary basins, *J. Geophys. Res.*, *99*, 20,051–20,058, 1994.
- Bradley, J. S., Abnormal formation pressure, *AAPG Bull.*, *59*, 957–953, 1975.
- Fowler, A.C., A compaction model for melt transport in the Earth's asthenosphere, Part I, the basic model, in *Magma Transport and Storage*, edited by M. P. Ryan, pp. 3–14, John Wiley, New York, 1990.
- Fowler, A.C., and X.-S. Yang, Fast and slow compaction in sedimentary basins, *SIAM J. Appl. Math.*, *59*, 365–385, 1998.
- Freeze, R.A., and J.A. Cherry, *Groundwater*, Prentice-Hall, Englewood Cliffs, N. J., 1979.
- Gibson, R. E., R. L. Schiffman, and K. W. Cargill, The theory of one-dimensional consolidation of saturated clays, II, Finite non-linear consolidation of thick homogeneous layers, *Can. Geotech. J.*, *18*, 280–293, 1991.
- Gratz, A.J., Solution-transfer compaction of quartzites — Progress towards a rate law, *Geology*, *19*, 901–904, 1991.
- Hedberg, H.D., Gravitational compaction of clays and shales, *Am. J. Sci.*, *184*, 241–287, 1936.
- Hunt, J. M., Generation and migration of petroleum from abnormally pressured fluid compartments, *AAPG Bull.*, *74*, 1–12, 1990.
- Keith, L. A., and J. D. Rimstidt, A numerical compaction model of overpressuring in shales, *Math. Geol.*, *17*, 115–135, 1985.
- Lahner, F. K., A model for intergranular pressure solution in open systems. *Tectonophysics.*, *245*, 153–170, 1995.
- McKenzie, D. P., The generation and compaction of partial melts, *J. Petrol.*, *25*, 713–765, 1984.
- Mudford, B. S., and M. E. Best, The Venture gas field, offshore Nova Scotia: A case study of overpressuring in a region of low sedimentation rate, *AAPG Bull.*, *73*, 1383–1396, 1989.
- Powley, D. E., Pressures and hydrogeology in petroleum basins, *Earth Sci. Revs.*, *29*, 215–226, 1990.
- Rutter, E.H., The kinetics of rock deformation by pressure solution, *Phil. Trans. Roy. Soc. London, Ser. A*, *283*, 203–219, 1976.
- Shi, Y., and C. Y. Wang, Pore pressure generation in sedimentary basins, overloading versus aquathermal, *J. Geophys. Res.*, *91*, 2153–2162, 1986.
- Skempton, A. W., Effective stress in soils, concrete and rocks, in *Pore Pressure and Suction in Soils*, pp. 4–16, Butterworth, London, 1960.
- Smith, J. E., The dynamics of shale compaction and evolution in pore-fluid pressures, *Math. Geol.*, *3*, 239–263, 1971.
- Tada, R., and R. Siever, Pressure solution during diagenesis, *Annu. Rev. Earth Planet. Sci.*, *17*, 89–118, 1989.
- Terzaghi, K., *Theoretical Soil Mechanics*, John Wiley, New York, 1943.
- Turcotte, D. L., and G. L. Schubert, *Geodynamics*, John Wiley, New York, 1982.
- Wangen, M., Pressure and temperature evolution in sedimentary basins, *Geophys. J. Int.*, *100*, 601–613, 1992.
- Weyl, P.K., Pressure solution and force of crystallisation — A phenomenological theory, *J. Geophys. Res.*, *64*, 2001–2025, 1959.
- Yang, X.S., Mathematical modelling of compaction and diagenesis in sedimentary basins, D. Phil. thesis, Oxford Univ., Oxford, England, 1997.

A. C. Fowler and X. S. Yang, Mathematical Institute, Oxford University, 24-29 St. Giles', Oxford, OX1 3LB, England. (e-mail: fowler@maths.ox.ac.uk; xinshe@maths.ox.ac.uk)

(Received February 18, 1998; revised August 20, 1998; accepted September 11, 1998.)